JOURNAL OF GAS TECHNOLOGY

Volume 8 /Issue 2/ Winter 2023 / Pages 56-73

Journal Home page: http://jgt.irangi.org

# Design and Simulation of Hydrogen Production from Diesel Reforming for Fuel Cell Applications

**Mostafa Jafari[1], Majid Khorshidian[2*], Mazaher Rahimi Esboee[3], Vahid Kord Firouzjaei[2], Ali Vatani[4]**

1. Researcher, Institute of Liquefied Natural Gas (I-LNG), School of Chemical Engineering, College of Engineering, University of Tehran, Tehran, Iran
2. Researcher, Malek Ashtar University of Technology, Northern Research Center for Science and Technology, Feridonkenar, Iran
3. Associate Professor, Malek Ashtar University of Technology, Northern Research Center for Science and Technology, Feridonkenar, Iran
4. Full Professor, Institute of Liquefied Natural Gas (I-LNG), School of Chemical Engineering, College of Engineering, University of Tehran, Tehran, Iran

## ARTICLE INFO

ORIGINAL RESEARCH ARTICLE

**Article History:**
Received: 09 October 2023
Revised: 12 November 2023
Accepted: 07 December 2023

**Keywords**:
Diesel
Reforming
Hydrogen
Fuel Cell
Electricity
Aspen HYSYS

DOR: 20.1001.1/jgt.2024.2030854.1040

## ABSTRACT

Hydrogen production encounters significant challenges in transportation and storage, such as leakage, transit safety, and the need for efficient storage conditions. On-site production through diesel fuel reforming presents a promising solution due to diesel's affordability, availability, and ease of transport. However, sulfur and carbon monoxide in diesel must be removed to protect the catalysts involved in the process. This study designs a conceptual process for reforming sulfur-containing diesel to generate 300 kW of electricity in a fuel cell system using the Douglas method, which structures chemical process design into a decision hierarchy. It starts with the Input-Output Structure, summarizing the process by detailing input and output streams based on designated design variables. The Recycle Stream Structure further divides the process into reactor and separation sections, each incorporating defined recycling flows. Finally, the Overall Separation Section Structure integrates gas and liquid recycling systems, providing a comprehensive strategy for separation unit design. The process flow diagram (PFD) was initially developed and subsequently analyzed in detail through simulation using Aspen HYSYS software. The results indicate that producing 300 kW of electricity requires 17 kg/h of pure hydrogen, which necessitates 47 kg/h of sulfur-free diesel. Overall, 60 kg/h of diesel is needed. Future research should focus on optimizing sulfur removal, reducing carbon monoxide levels, enhancing the water-gas shift reaction, maximizing energy efficiency, and assessing economic viability, including ROI and payback period.

**How to cite this article**
M. Jafari, M. Khorshidian, M. Rahimi Esboee, V. Kord Firouzjaei, A. Vatani, Design and Simulation of Hydrogen Production from Diesel Reforming for Fuel Cell Applications. Journal of Gas Technology. 2023; 8(2): 56-73. ( https://jgt.irangi.org/article_714881.html )

* Corresponding author.
E-mail address: khorshidian@mut.ac.ir, (M. Khorshidian).

Available online 31 December 2023

## 1. Introduction

Producing and exporting hydrogen on-site is a significant challenge(Jafari, Deljoo, et al., 2020). Using liquid fuels in fuel cell systems expands the potential for deploying this technology in regions lacking readily available infrastructure for hydrogen production or facing difficulties in hydrogen due to volume constraints or transportation challenges (Le et al., 2023). Consequently, reforming liquid fuels emerges as a viable solution for global hydrogen production, considering the greater convenience and cost-effectiveness of exporting liquid products (Jafari, Vatani, et al., 2021; Lindström et al., 2009). Numerous researchers view hydrogen production from liquid fuels (such as diesel, kerosene, biodiesel, methanol, ethanol, etc.) as a promising midterm option (Dawood et al., 2020; Ghasemzadeh et al., 2017). Considering the complexities associated with the composition of diesel fuel and the challenges posed by numerical simulations in modeling various components and chemical reactions involved in diesel fuel reforming, it becomes necessary to employ rational and simplifying approximations. In this regard, (Table 1) presents a compilation of essential compounds utilized in simulations or models as surrogates for diesel fuel. Sulfur compounds in diesel act as a poison for fuel cell catalysts (platinum) and steam reforming catalysts (nickel) (Hoguet et al., 2009). (Table 2) shows the common sulfur compounds in diesel fuel and their weight percentages. Sulfur compounds are deemed the most significant impurities in diesel fuel.

**Table 1. List of Compounds Used in Diesel Reforming Process**

| Chemical formula | Reference | Chemical formula | Reference |
|---|---|---|---|
| $C_{13.88}H_{24.053}$ | (Lindström et al., 2009) | $C_{14}H_{26}$ | (Creaser et al., 2011) |
| $C_{17}H_{36}$ - $C_{19}H_{38}$ | (Samsun et al., 2020) | $C_{11.6}H_{19.6}$ | (M. Bae et al., 2021) |
| $C_{12}H_{20}$ | (Fauteux-Lefebvre et al., 2011) | $C_{13.4}H_{24.7}$ | (Samsun et al., 2015) |
| $C_{14.342}H_{24.75}O_{0.0495}$ | (Sahin, 2008) | $C_{12}H_{23}$ | (Wang et al., 2021) |
| $C_{13.75}H_{27.14}$ | (Brown, 2001) | $C_{12}H_{26}$ | (J. Bae et al., 2016) |
| $C_{16.2}H_{30.6}$ | (Lindermeir et al., 2007) | $C_{14}H_{26}$ | (Dolanc et al., 2016) |
| $C_{13.3}H_{24.7}$ | (Martin et al., 2015) | $C_{16}H_{34}$ | (Liu et al., 2004) |

**Table 2. Common Sulfur Compounds and Mass Fraction in Diesel Fuel**

| Chemical formula | Mass Fraction | Reference |
|---|---|---|
| Dibenzothiophene (DBT) | 0.012 | (Jafari & Garakani, 2021; Permatasari et al., 2016) |
| Dibenzothiophene (DBT) | 0.015 | (Jafari & Khalili-Garakani, 2021; Pereira et al., 2000) |
| 4,6-Dimethyldibenzothiophene (4,6-DMDBT) | - | (Kaila et al., 2008) |
| Dibenzothiophene (DBT) | 0.014 | (Gonzalez et al., 2018) |

(Amphlett et al., 1998) simulated a 250-kW diesel fuel processor/PEM fuel cell system. They developed a process simulation model incorporating a higher temperature model for liquid hydrocarbon fuels and a steady-state electrochemical fuel cell model. Their investigation assessed the system's performance under various conditions and conducted a

preliminary assessment of thermal integration issues. (Ersoz et al., 2006) Three reforming technologies (steam reforming, partial oxidation, and autothermal reforming) were compared for hydrogen production from fossil fuels for PEM fuel cells. They studied 100-kW PEM fuel cell systems using natural gas, gasoline, and diesel, aiming to assess their overall efficiency. The study highlighted steam reforming as the most efficient fuel preparation option, with natural gas and steam reforming showing the highest fuel cell system efficiency. (Samsun et al., 2015), Investigated reforming diesel and jet fuel for fuel cells at a systems level. They focused on steady-state and transient operations of a 28-kWh fuel processor, addressing complexities and stability issues. Their results demonstrated high conversion efficiencies and effective CO management, enhancing the application of fuel cell technology in auxiliary power units and remote power systems. (Wang et al., 2021) studied a new SOFC-CCHP system fueled by diesel reforming with chemical looping hydrogen generation. Using Aspen software and a FORTRAN program, they analyzed system performance, achieving a power efficiency of 54.1% and identifying peak values for critical parameters. These findings lay the groundwork for future diesel-based energy systems, offering energy-saving and carbon recovery optimization insights. (Ješić et al., 2022), Conducted a computational investigation into diesel's auto-thermal reforming (ATR) process for hydrogen production, aiming to support PEM fuel cell applications. The study validated product composition through Gibbs minimization and investigated various parameters, including heat input, pressure potential, feed ratios, and kinetic parameters from the literature. Their findings facilitate the successful design and operation of ATR processes by enhancing the understanding of thermodynamic equilibria, transport phenomena, and mechanistic chemical rates.

(Geng et al., 2023) investigated the co-reforming of diesel and methanol into hydrogen-enriched gases for solid oxide fuel cell applications. They used Ru/γ-$Al_2O_3$ and Ni/γ-$Al_2O_3$ catalysts for steam reforming of diesel, achieving 100% diesel conversion and high hydrogen selectivity at temperatures above 600 °C. While the Ni/γ-$Al_2O_3$ catalyst showed poor carbon tolerance, adding methanol to the steam-diesel mixture extended the process life from 120 to 600 hours at 750 °C. The reformed diesel gas (RDG) fed into a solid oxide fuel cell (SOFC) achieved a peak power density of 1.34 W/$cm^2$ at 750 °C, with stable cell voltage and no carbon deposition on the Ni-YSZ anode, demonstrating RDG's suitability as a fuel for SOFC applications.

The production of hydrogen from diesel reforming for fuel cell applications is feasible and can be optimized using various reforming techniques and simulation tools. Proper control of operating parameters and efficient thermal integration are crucial for maximizing hydrogen yield and system efficiency. This study identifies research gaps in diesel fuel reforming for electricity generation in fuel cell systems, particularly at low capacities. Despite existing advancements, crucial areas have yet to be thoroughly explored. One significant gap is the effective removal of sulfur from diesel fuel, which is essential for preventing fuel cell catalyst poisoning. Additionally, there is a need for an integrated approach that combines both design and simulation to optimize the efficient conversion of sulfur-containing diesel into electricity. Our research aims to address these gaps by developing a comprehensive Process Flow Diagram (PFD) for steam-reforming diesel to produce hydrogen, which will be used to power a 300-kW fuel cell system. The novelty of our study lies in its detailed focus on sulfur removal and the subsequent integration of design and simulation processes. After synthesizing the PFD, we will thoroughly examine and simulate the process using Aspen HYSYS software to ensure optimal performance and efficiency.

## 2. Conceptual Design

Conceptual design in diesel steam reforming is crucial for creating an efficient blueprint for hydrogen production. It establishes optimal process flow diagrams and refines operating conditions, paving the way for effective implementation and resource utilization. The Douglas method's decision-making hierarchy guides this process through four key steps: evaluating process continuity, defining input and output streams, structuring recycled streams, and outlining separation section strategies (Douglas, 1988).

### 2.1. Input Information

The initial data emphasizes the conditions required for diesel steam reforming reactions. Key processes include hydrodesulfurization (HDS) and the pre-reforming reaction (PREF). (Tables 3 & 4) outline the design parameters, process inputs, and diesel composition. Estimating hydrogen consumption is critical for producing 300 kW of electricity.

**Table 3. Design Conditions and Input Information**

| Parameters | Value |
|---|---|
| Power Generation (kW) | 300 |
| Operating Pressure (bar) | 30 |
| HDS Reactor Outlet $H_2S$ Concentration (ppm) | <5 |
| **Requirements for Purified Hydrogen Stream** | |
| Water (µmol/mol) | 5 |
| Total Hydrocarbons (µmol/mol) | 2 |
| Oxygen (µmol/mol) | 5 |
| $CO_2$ (µmol/mol) | 2 |
| CO (µmol/mol) | 0.2 |
| Total Sulfur (µmol/mol) | 0.004 |

**Table 4. Condition and Composition of Sour-Diesel**
(Permatasari et al., 2016)

| Properties | Value |
|---|---|
| Stream Name | Sour-Diesel |
| Temperature (°C) | 25 |
| Pressure (bar) | 1.013 |
| Component | Mass Fraction |
| (DBT) | 0.0150 |
| Naphthalene | 0.0080 |
| n-$C_{16}H_{34}$ | 0.9050 |

The HDS reaction operates at 200-300 °C temperatures 1-18 MPa pressures using NiMo/$Al_2O_3$ or CoMo/$Al_2O_3$ catalysts in a packed-bed reactor (Jejurkar et al., 2020). The PREF reaction occurs at 500-550 °C and 2-5 MPa, using Ni/$Al_2O_3$ catalysts in an adiabatic fixed-bed reactor (Ramantani et al., 2022). Steam methane reforming (SMR) reactions are crucial for hydrogen production, operating at 700-850 °C and 2-5 MPa (Cherif et al., 2021). The output of the SMR reactor enters the water-gas-shift (WGS) reactor to enhance hydrogen production. Typically, WGS processes encompass high-temperature (300-450 °C) and low-temperature (200-250 °C) stages, employing Fe-Cr and Cu-Zn-Al catalysts, respectively (Lee et al., 2023).

Given CO's detrimental effect on precious metal catalysts in fuel cells, Preferential Oxidation (PROX) reactions (120-160 °C) are implemented to eliminate CO, utilizing catalysts like platinum or copper supported by high-surface-area metal oxides such as alumina ($Al_2O_3$) or cerium ($CeO_2$) (Davǫ-Quiǫonero et al., 2020). The reforming furnace generates heat for steam production and heating the PREF reactor's outlet stream to attain the SMR reactor's reaction temperature. Its primary products include water, carbon dioxide, and heat, with reactions R9, R10, and R11 assumed to achieve complete conversion. (Table 5) details stoichiometry, reaction rates, and kinetics for the involved reactions.

**Table 5. Stoichiometry and Reaction Rates of Synthetic Reactions in Diesel Reforming Processes**

| Parameters | Specification |
|---|---|
| HDS (R1) Stoichiometry | $C_{12}H_8S + H_2 \rightarrow C_{12}H_{10} + H_2S$ |
| HDS (R1) Kinetic Data | $r_i = A_i.\exp\left(\frac{-E_i}{RT}\right).C^1_{C_{12}H_8S}$ |
| | $r_i = \frac{kmol}{m^3.S}$ , $A_i = 2.9 \times 10^7 \frac{1}{s}$ , $E_i = 8.7 \times 10^4\ kJ/k\,mole$ |
| PREF (R2) Stoichiometry | $C_{16}H_{34} + 16H_2O \rightarrow 33H_2 + 16CO$ |
| PREF (R2) Kinetic Data | $r_i = A_i.\exp\left(\frac{-E_i}{RT}\right).C^1_{C_{16}H_{34}}.C^1_{H_2O}$ |
| | $r_i = \frac{kmol}{m^3.S}$ , $A_i = 2.01 \times 10^9 \frac{m^3}{kmole.s}$ , $E_i = 116.9\ kJ/m\,ole$ |
| PREF (R3) Stoichiometry | $C_{10}H_8 + 10H_2O \rightarrow 10CO + 14H_2$ |
| PREF (R3) Kinetic Data | $r_i = A_i.\exp\left(\frac{-E_i}{RT}\right).C^1_{C_{10}H_8}\,C^1_{H2O}$ |
| | $r_i = \frac{kmol}{m^3.S}$ , $A_i = 10000\ \frac{m^3}{kmole.s}$ , $E_i = 118\ kJ/m\,ole$ |
| PREF (R4) Stoichiometry | $CO + 3H_2 \rightarrow CH_4 + H_2O$ |
| PREF (R4) Kinetic Data | $r_i = A_i.\exp\left(\frac{-E_i}{RT}\right).C^1_{CO}$ |
| | $r_i = \frac{kmol}{m^3.S}$ , $A_i = 1 \times 10^9 \frac{1}{s}$ , $E_i = 100\ kJ/m\,ole$ |
| PREF (R5) Stoichiometry | $C_{12}H_{10} + 12H_2O \rightarrow 12CO + 17H_2$ |
| PREF (R5) Kinetic Data | $r_i = A_i.\exp\left(\frac{-E_i}{RT}\right).C^1_{C_{12}H_{10}}\,C^1_{H2O}$ |
| | $r_i = \frac{kmol}{m^3.S}$ , $A_i = 11500\ \frac{m^3}{kmole.s}$ , $E_i = 135\ kJ/m\,ole$ |
| SMR (R6) Stoichiometry | $CH_4 + H_2O \rightarrow CO + 3H_2$ |
| SMR (R6) Kinetic Data | $r_i = A_i.exp\left(\frac{-E_i}{RT}\right).C^1_{CH_4}\,C^1_{H_2O}$ |
| | $r_i = \frac{kmol}{m^3.S}$ , $A_i = 2.9 \times 10^7 \frac{1}{s}$ , $E_i = 8.7 \times 10^4\ kJ/k\,mole$ |
| WGS (R7) Stoichiometry | $CO + H_2O \rightarrow CO_2 + H_2$ |
| WGS (R7) Kinetic Data | $r_i = A_i.exp\left(\frac{-E_i}{RT}\right).C^1_{CO}\,C^1_{H_2O}$ |
| | $r_i = \frac{kmol}{m^3.S}$ , $A_i = 1.4 \times 10^5 \frac{m^3}{kmole.s}$ , $E_i = 54\ kJ/m\,ole$ |
| PROX (R8) Stoichiometry | $2CO + O_2 \rightarrow 2CO_2$ |
| PROX (R8) Kinetic Data | $r_i = A_i.\exp\left(\frac{-E_i}{RT}\right).C^1_{CO}$ |
| | $r_i = \frac{kmol}{m^3.S}$ , $A_i = 8 \times 10^7 \frac{1}{s}$ , $E_i = 80\ kJ/m\,ole$ |
| R9 Stoichiometry | $2C_{16}H_{34} + 49O_2 \rightarrow 34H_2O + 32CO_2$ |
| R10 Stoichiometry | $C_{10}H_8 + 12O_2 \rightarrow 4H_2O + 10CO_2$ |
| R11 Stoichiometry | $2C_{12}H_{10} + 29O_2 \rightarrow 10H_2O + 24CO_2$ |

## 2.2. Input-Output Structure

The input-output structure flowchart needs to be determined in the second stage of the conceptual process design for diesel steam reforming (Figure 1). A process box is drawn, focusing on inputs and outputs without considering other details. To define this box, it is necessary to answer questions about inputs, main and by-products, and other relevant details. Six fundamental questions must be addressed in the next stage to complete the inputs and outputs based on design variables. One of these questions examines the need for feed purification and the presence of recyclable by-products. For instance, sulfur compounds in diesel must be removed to ensure system stability and optimal performance.

Additionally, recyclable by-products are usually not recycled in steam reforming hydrogen production processes due to price differences and the return stream's importance, improving process efficiency and costs. In the HDS unit, there is no purge flow due to two factors. First, for a return and purge flow, at least one reaction product must be light invalid in HDS. Second, the required hydrogen is supplied from the downstream process, and since it is free of hydrogen sulfide, the condition for a purge is not met. Therefore, there is no purge flow in the reforming process, and hydrogen goes to the recycling process. According to (Table 6), there will be four output streams and one recycle stream.

**Table 6. Determining Output Flows, Recycle, and Purge**

| Component | NBP (°C) | Stream |
|---|---|---|
| $H_2$ | -252.8 | Primary Product and Recycle |
| $H_2$ | -252.8 | Recycle |
| $CO_2$ | -78.55 | Waste |
| $H_2S$ | -56.65 | Waste |
| $H_2O$ | 100 | Waste |

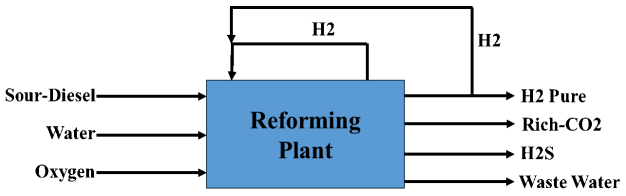


**Figure 1. The Input-Output Structure of the Diesel Reforming Process**

## 2.3. Recycle Structure

In the third step of the conceptual design of diesel reforming, critical decisions are made regarding the structure of return streams in the flowchart. This includes determining the number of reactor systems based on assessing reaction conversion levels, reaction types, and intensities, among other factors. The number of recycle streams is also determined by calculating the required stoichiometry. If the stoichiometry exceeds the required amount, additional input to the reactor may be necessary to maintain environmental equilibrium. Furthermore, if gas compression is needed for recycling streams or other purposes, a gas compressor may be required, with its costs typically estimated based on energy consumption requirements.

In the process, only the reactant recycled after purification is in the HDS reactor, which requires a compressor. This compressor increases the hydrogen pressure from 28.5 bar (Pressure of the hydrogen recovery unit by amine method) to 32.5 bar (input to the HDS reactor). Then, the stream enters the cooler for temperature adjustment. The produced hydrogen also supplies part of the required hydrogen. Two compressors are needed in this process, with the second compressor operating at a lower capacity than the first. The amine unit recovers most of the hydrogen needed for the HDS reactor. The type of reactor operation may necessitate adiabatic or non-adiabatic operation, depending on the need for precise temperature control in the reactor. (Figure 2) shows the recycle stream structure in the diesel reforming process.

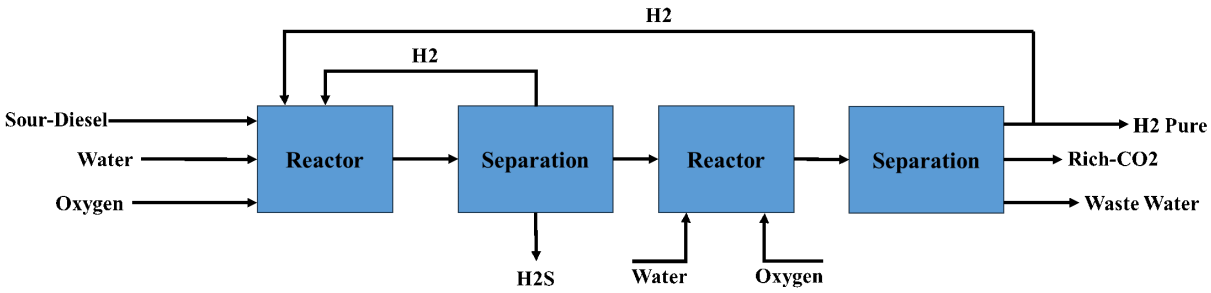


**Figure 2. Recycle Stream Structure in the Diesel Reforming Process**

The most important design variables in the diesel reforming process include the conversion percentage of the limiting reactant in the HDS, PREF, SMR, WGS, and PROX reactors, as well as the furnace; the molar ratio of the reactants; and the temperature and Pressure of the reactors. The hydrogen-to-oil ratio is considered to be 150 $m^3/m^3$ (Awad et al., 2020), calculated using Aspen HYSYS software (the molar ratio of hydrogen to diesel is 1.5 to 2.5). The oxygen-to-CO molar ratios in the PROX reactor are between 0.5 and 1 (Castaldi, 2009).

Reaction R1 occurs in the HDS reactor, reactions R2 to R5 in the PREF reactor, reaction R6 in the SMR reactor, the high-temperature WGS in an HTS reactor, the low-temperature WGS in an LTS reactor, and reaction R8 in a PROX reactor. Reactions R9 to R11 occur in the furnace, totaling seven reactors. (Figure 3) illustrates the number of reactors involved in the diesel reforming process.

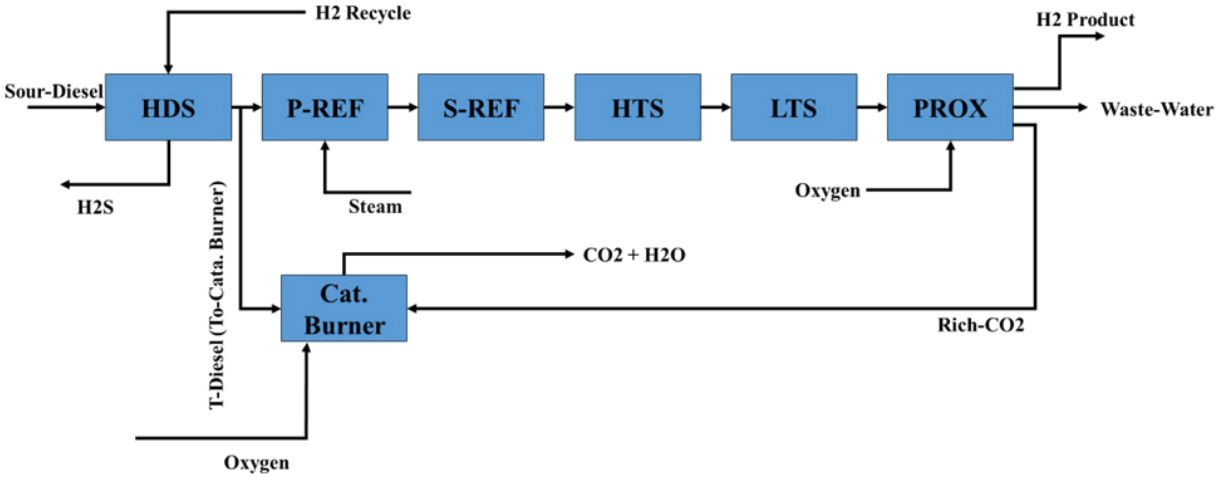


**Figure 3. The Number of Reactors in the Diesel Reforming Process**

## 4.1. Static Simulation

The fourth step in conceptual diesel reforming design, known as separation design, involves three main components: general structure, gas separation, and liquid separation. It establishes an overall separation framework based on the diverse states of the reactor output stream (liquid, vapor, or liquid-vapor mixture). Decisions on system configuration are guided by the phase of the reactor output, specifying methods for gas and liquid separation and detailing necessary tools and processes. Gas separation aims to isolate the gas phase, requiring the identification of appropriate tools such as two-phase separators, solid separators, or distillation towers. The HDS reactor output turns into a two-phase mixture after cooling

to 65 ℃, initially processed in a flash vessel or separator. At 120 ℃ and 24 bars, the PROX reactor output is released as a two-phase flow, then separated in a two-phase separator. Hydrogen gas and carbon dioxide are separated from the water-containing liquid stream.

The vapor separation system is designed using post-flash calculations to identify the vapor phase and then devise the vapor recovery system. The optimal placement and cost-effective type of vapor recovery system are determined by evaluating four potential scenarios: 1) in the Purge stream, 2) in the Recycle stream, 3) in the output vapor stream from the Flash, or 4) not needed. The steam exiting the first two-phase separator after the PROX reactor typically contains valuable hydrogen compounds and hydrogen sulfide, which must be separated. Since there is no Purge system, the gas recovery system is placed in the Recycle stream. Hydrogen recovery for return to the HDS reactor is done using the amine purification method with MDEA solvent, where hydrogen gas containing hydrogen sulfide is chemically absorbed in a tower with MDEA solution.

The liquid separation system design involves decisions on removing light components to maintain product quality, determining their destination, exploring azeotrope recycling, solvent use for breaking azeotropic points, assessing distillation feasibilities and column sequences, and exploring alternative methods if distillation is not viable. (Table 7) shows molar percentages of light components, indicating heavier diesel components causing light products to dissolve, prompting separation to remove hydrogen and hydrogen sulfide. While a two-phase separator can separate light components from liquids, vaporization of valuable components suggests that separating light components from liquids is preferable. After complete feedstock consumption and 100% conversion in the reactor, the light gas stream contains $H_2$ and $H_2S$. Distillation towers separate these compounds, with hydrogen extracted at the tower top due to its lighter nature. This purified hydrogen is crucial for fuel cell systems. Palladium membranes, known for their high selectivity in separating hydrogen from impurities like $CO_2$, are employed for this purpose. These membranes allow unhindered hydrogen passage while blocking other gases, ensuring cost-effective and efficient single-stage purification, which is essential for high-purity hydrogen processes. (Table 9) provides specifications of palladium membranes.

**Table 8. Mole Fraction of Liquid Stream Post-HDS Reactor Two-phase Separator**

| Component | NBP | Mole Fraction |
|---|---|---|
| Hydrogen | -252.6 | 0.0151 |
| $H_2S$ | -59.7 | 0.0052 |
| $H_2O$ | 100 | 0.0007 |
| Naphthalene | 218.0 | 0.1299 |
| BiPhenyl | 255.0 | 0.0169 |
| n-C16 | 286.8 | 0.8332 |
| DiBZThiphene | 331.5 | 0.0000 |

**Table 9. Palladium Membrane Specifications (Jafari, Deljoo, et al., 2020)**

| Specification | Value | unit |
|---|---|---|
| $CH_4$ permeance | 1.00E-19 | mol/m$^2$.s.pa |
| $H_2$ permeance | 2.80E-04 | mol/m$^2$.s.pa |
| $O_2$ permeance | 5.50E-18 | mol/m$^2$.s.pa |
| $N_2$ permeance | 3.00E-17 | mol/m$^2$.s.pa |
| $CO_2$ permeance | 1.00E17- | mol/m$^2$.s.pa |
| $H_2O$ permeance | 5.00E21- | mol/m$^2$.s.pa |

## 3. Simulation Strategy

The simulation process was conducted using Aspen HYSYS v.12, considering various kinetic models for the primary components of the studied operating system. Additional software, such as PRO/II, had to be employed to simulate the membrane purification section, and its results were integrated into the Aspen simulation. An important step in the simulation is the selection of units (Ghasemzadeh et al., 2017), in which the Euro SI unit has been used. The fluid package employed in this simulation is the Acid Gas equation (Jafari, Sarrafzadeh, et al., 2021); however, certain units require the definition of a separate fluid package for the simulation to be performed with very high accuracy (Jafari, Sarrafzadeh, et al., 2021). In the steam reforming section and fuel cell unit, the PRSV fluid package has been utilized (Jafari, Sarrafzadeh, et al., 2020). The simulation assumptions are as follows:

- Diesel Composition: Simplified to a single hydrocarbon, aromatic, naphthenic, and sulfur compound to reduce computational complexity.
- HDS Reactor Side Reactions: Side reactions are neglected to focus on the primary hydrogenation reaction, simplifying the model.
- HDS Reactor Modeling: Assumed to be a single tubular reactor with catalyst, instead of multi-stage catalytic beds, for reduced complexity.
- Reforming Furnace: Complete combustion reactions are assumed in a conversion reactor to achieve precise results.
- Reforming and Pre-Reforming: Both reactions occur in a single tubular reactor, simplifying the process and reducing computational complexity.
- Membrane Purification Unit: Simulated using Component Splitter in Aspen HYSYS, with membrane performance calculated in ProII and data imported to HYSYS.
- Hydrogen Stream for Fuel Cell: Pure hydrogen stream at 7.88 kmol/hr with required air enters the fuel cell system, with 80% hydrogen conversion and adjusted oxygen consumption for optimal performance.

## 4. Results and Discussion

With hydrogen's Lower Heating Value (LHV) at 120,000 kJ/kg (33.33 kWh/kg) and fuel cell efficiencies ranging from 40% to 60%, approximately 9 to 14.5 kg/h of pure hydrogen is required. Purifying hydrogen using a membrane process, with a recovery rate of 85% to 90%, is vital. Producing 17 kg/h of hydrogen necessitates approximately 42.5 kg/h of diesel. Moreover, purified diesel will be used for heat in the furnace, totaling over 45 kg/h. Precise calculations in Aspen HYSYS, assuming an additional 50-55% diesel consumption for the furnace, estimate a total input of 65-70 kg/h of diesel with sulfur compounds. In the HDS reactor, the hydrogen recycle stream is crucial, mostly recovered from the HDS unit, with some supplemented by in-process hydrogen. A compressor is necessary to return hydrogen due to pressure and temperature adjustments. Two compressors are needed, with the second operating at a lower capacity. Compressor costs include installation, operation, maintenance, energy consumption, and performance-related expenses. For the HDS reactor, hydrogen availability is 0.55 kilomoles per hour at 2.4 bar and 0.8 kW power. The second compressor receives 0.0172 kilomoles per hour at 1 bar pressure, with a flow of 0.97 cubic meters per hour, increasing to 27.90 bar with 0.96 kW power.

Since the pre-reforming reactor's outlet temperature is lower than the SMR reactor, the pre-reforming reactor's outlet temperature

needs to increase before entering the SR reactor. Hence, a heat transfer device is needed between the pre-reforming and reforming methane reactors for heating. This heat will be provided by passing the pre-reforming reactor's outlet stream through the reforming furnace. The output stream from the reforming reactor enters the HTS and LTS reactors. These reactors also operate adiabatically, with the HTS reactor's inlet temperature at 300 °C and the LTS reactor at 200 °C. Finally, the PROX reactor also operates adiabatically, with an inlet temperature of 120 °C. With these interpretations, after the steam-methane reformer, the outlet streams must be cooled before entering the HTS, LTS, and PROX reactors. Cooling water will be used in heat exchangers for cooling these streams (Figure 4).

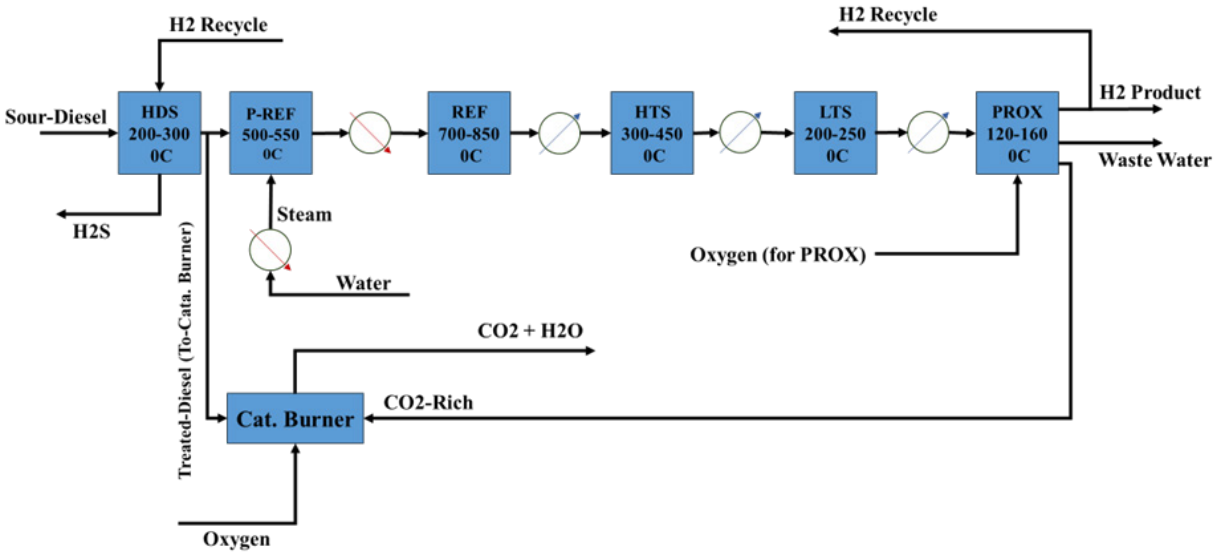


**Figure 4. Reactor Sections and Temperature Ranges**

A distillation column is used to separate $H_2S$ from diesel fuel. In fuel cell systems, it is crucial to extract pure, impurity-free hydrogen from the reformer gas streams to ensure the longevity of the fuel cell. The quality of hydrogen must be guaranteed according to the international standards ISO 14687-2:2012 and ISO/DIS 19880-8 (Bacquart et al., 2019). Using palladium membranes to purify hydrogen from $CO_2$-rich streams is valued for its cost-effectiveness, efficiency, and single-step process. This method is essential for industries needing high-purity hydrogen, improving process quality and efficiency. This section analyzes heat transfer equipment and temperature adjustment requirements, including the placement of heat exchangers. In the HDS reactor, the output cools to 65 °C, becoming biphasic, and enters a flash vessel. Cooling is achieved with water at 26 °C inlet and 31 °C outlet temperatures. Using Aspen software, the coolant flow rate is calculated. This coolant then cools the condensers in the hydrogen recovery and separation towers. Each tower has reboilers heated by LP and HP steam. The treated diesel flows into the pre-reforming reactor, with some entering a catalytic furnace to produce steam. The furnace generates LP, MP, and HP steam, which heat the prereformer's endothermic reaction. Methane reforming reactor input is at 850 °C and output at 550 °C, needing cooling to 450 °C for the WGS reactor, using 26 °C coolant water exiting at 31 °C. LTS reactors at 200 °C and PROX reactors at 160 °C also require heat exchangers. Finally, the PROX reactor output is cooled to 50 °C for water separation before membrane processing. (Figure 4) illustrates the process flow diagram for steam diesel reforming.

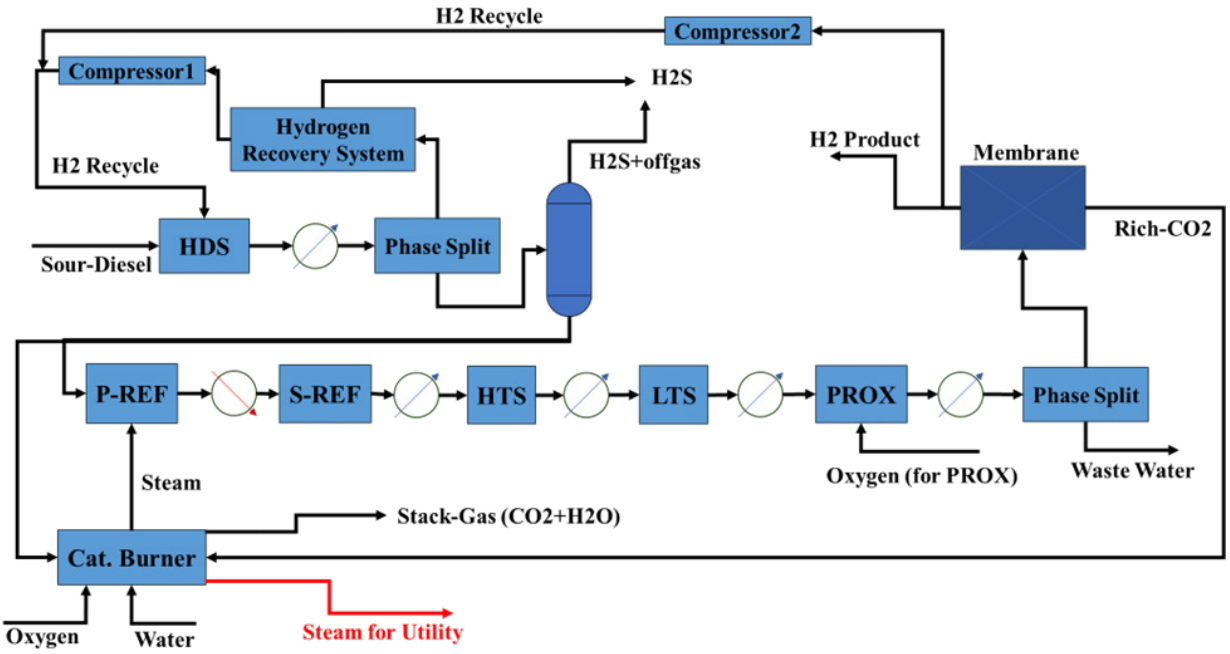


**Figure 5. Process Flow Diagram of Diesel Steam Reforming**

The simulation schematics of the final HDS unit and the hydrogen recovery unit in the amine solvent-based hydrogen sweetening unit are shown in (Figures 6, 7 and 8). In this simulation, the diesel stream undergoes hydrodesulfurization in the HDS reactor. Then, the hydrogen used in this process is introduced into the sweetening process via an amine solvent for recovery and reuse. The desulfurized diesel, primarily free of sulfur compounds like dibenzothiophene, enters the steam reformer reactor.

Both high-temperature and low-temperature shift reactions are conducted to enhance the quality of the syngas. Increasing the $H_2$/CO ratio directs the gas to the PROX reactor, converting CO to $CO_2$. The output stream from the PROX reactor subsequently enters the membrane process to produce pure hydrogen. The pure hydrogen is fed into the fuel cell system to generate electricity. (Table 10) summarizes the input and output streams for converting sulfur-containing diesel fuel into pure hydrogen and then converting hydrogen into electricity in the fuel cell system. (Table 11) shows the utility consumption and net electricity produced.

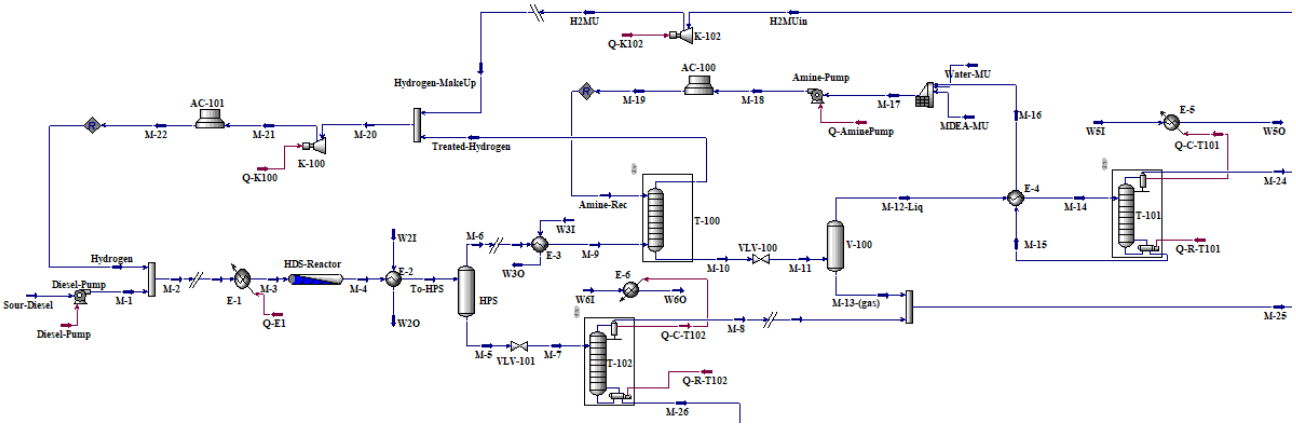


**Figure 6. Schematic Simulation of the HDS Process with Hydrogen Gas Recovery**

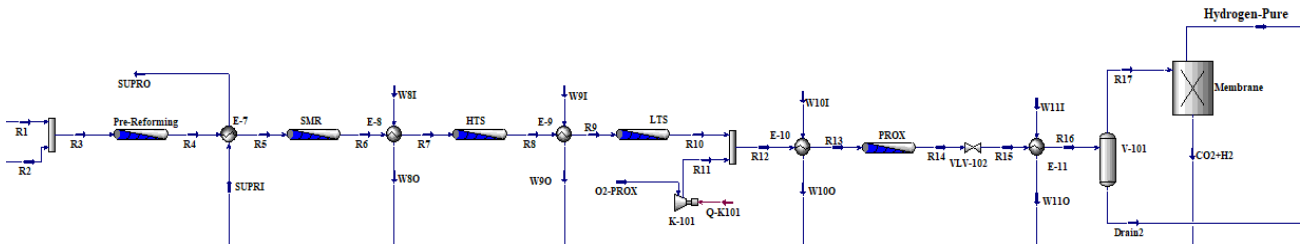


**Figure 7. Schematic Simulation of the Diesel Reforming Process with Hydrogen Purification**

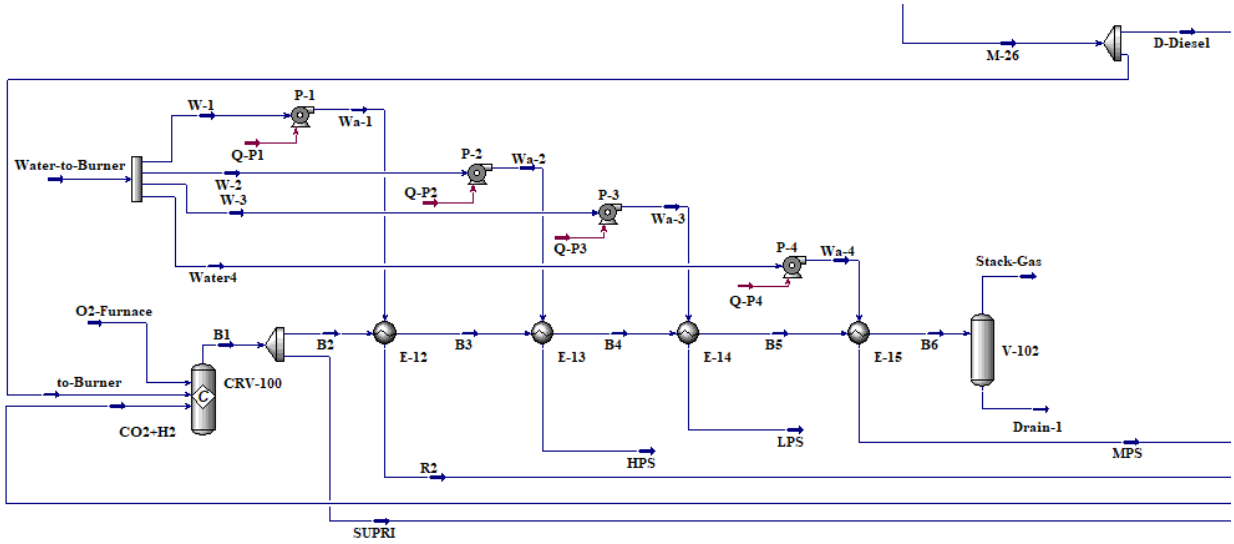


**Figure 8. Schematic Simulation of the Reforming Furnace Section**

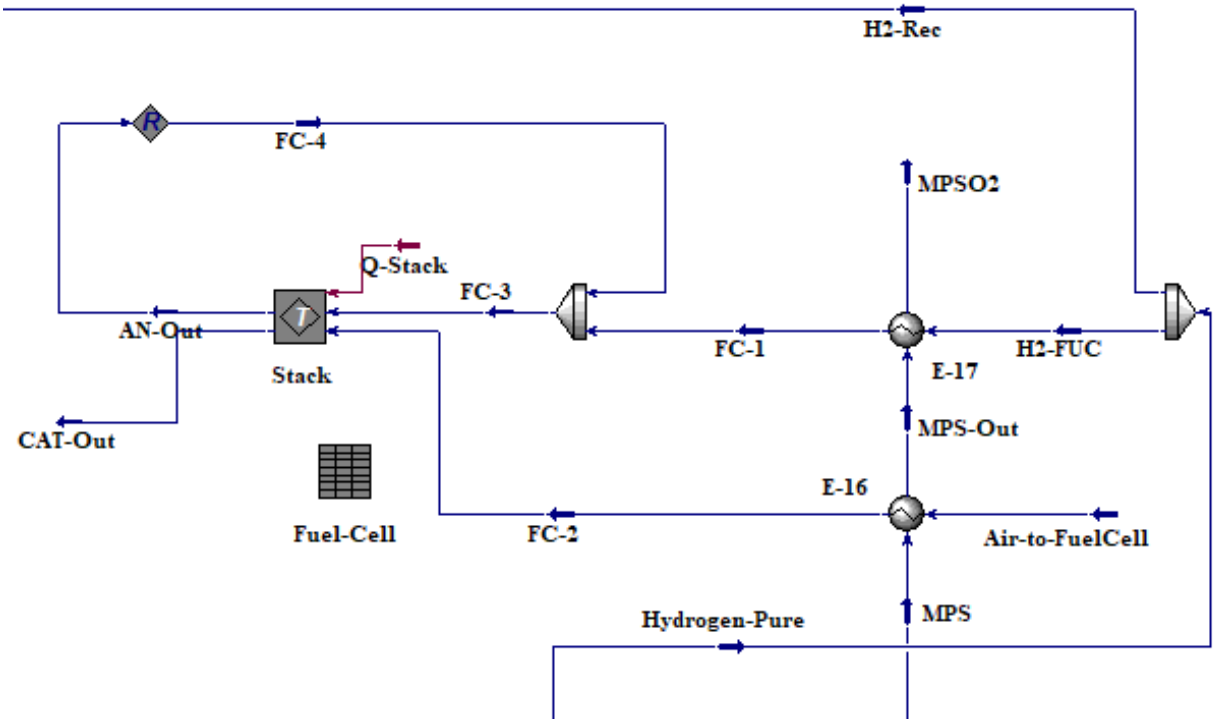


**Figure 9. Schematic Simulation of the Fuel-Cell Section**

**Table 10. Summary of the Input and Output streams of Sour-Diesel Fuel to Power process**

| | Sour-Diesel | Hydrogen | M-4 | Amine-Rec | Treated-Hydrogen | M-24 | M-26 | D-Diesel | to-Burner |
|---|---|---|---|---|---|---|---|---|---|
| Vapor Fraction | 0 | 1 | 1 | 0 | 1 | 1 | 0 | 0 | 0 |
| Temperature (°C) | 25 | 25 | 251 | 45 | 45 | 87 | 266 | 266 | 266 |
| Pressure (bar) | 1.0 | 32.0 | 30.5 | 29.4 | 28.9 | 1.2 | 1.1 | 1.1 | 1.1 |
| Molar flow (kgmole/h) | 0.30 | 0.50 | 0.79 | 1.00 | 0.48 | 0.01 | 0.30 | 0.22 | 0.07 |
| Mass Flow (kg/h) | 63.00 | 1.04 | 64.03 | 29.17 | 1.00 | 0.21 | 62.71 | 47.00 | 15.71 |
| Comp Mole Frac (Naphthalene) | 0.13 | 0.00 | 0.05 | 0.00 | 0.00 | 0.00 | 0.13 | 0.13 | 0.13 |
| Comp Mole Frac (n-C16) | 0.85 | 0.00 | 0.32 | 0.00 | 0.00 | 0.00 | 0.85 | 0.85 | 0.85 |
| Comp Mole Frac (DBT) | 0.02 | 0.00 | 0.00 | 0.00 | 0.00 | 0.00 | 0.00 | 0.00 | 0.00 |
| Comp Mole Frac (Hydrogen) | 0.00 | 1.00 | 0.62 | 0.00 | 1.00 | 0.01 | 0.00 | 0.00 | 0.00 |
| Comp Mole Frac ($H_2S$) | 0.00 | 0.00 | 0.01 | 0.00 | 0.00 | 0.46 | 0.00 | 0.00 | 0.00 |
| Comp Mole Frac ($H_2O$) | 0.00 | 0.00 | 0.00 | 0.89 | 0.00 | 0.53 | 0.00 | 0.00 | 0.00 |
| Comp Mole Frac (MDEA) | 0.00 | 0.00 | 0.00 | 0.11 | 0.00 | 0.00 | 0.00 | 0.00 | 0.00 |
| Comp Mole Frac (BiPhenyl) | 0.00 | 0.00 | 0.01 | 0.00 | 0.00 | 0.00 | 0.02 | 0.02 | 0.02 |
| | **R1** | **R2** | **R10** | **$O_2$-PROX** | **R16** | **Hydro-gen-Pure** | **$CO_2$+$H_2$** | **Air-to-FuelCell** | **CAT-Out** |
| Vapor Fraction | 0 | 1 | 1 | 1 | 1 | 1 | 1 | 1 | 1 |
| Temperature (°C) | 268 | 750 | 202 | 25 | 50 | 50 | 65 | 50 | 190 |
| Pressure (bar) | 30.0 | 30.0 | 28.4 | 1.0 | 10.9 | 1.0 | 11.0 | 1.0 | 1.0 |
| Molar flow (kgmole/h) | 0.22 | 7.83 | 14.37 | 0.16 | 14.37 | 8.33 | 4.53 | 28.09 | 33.92 |
| Mass Flow (kg/h) | 47.00 | 141.00 | 188.01 | 5.03 | 193.03 | 16.79 | 147.86 | 810.66 | 834.15 |
| Comp Mole Frac (Naphthalene) | 0.13 | 0.00 | 0.00 | 0.00 | 0.00 | 0.00 | 0.00 | 0.00 | 0.00 |
| Comp Mole Frac (n-C16) | 0.85 | 0.00 | 0.00 | 0.00 | 0.00 | 0.00 | 0.00 | 0.00 | 0.00 |
| Comp Mole Frac (Hydrogen) | 0.00 | 0.00 | 0.66 | 0.00 | 0.66 | 1.00 | 0.25 | 0.00 | 0.00 |
| Comp Mole Frac (Oxygen) | 0.00 | 0.00 | 0.00 | 1.00 | 0.00 | 0.00 | 0.00 | 0.21 | 0.00 |
| Comp Mole Frac (Nitrogen) | 0.00 | 0.00 | 0.00 | 0.00 | 0.00 | 0.00 | 0.00 | 0.77 | 0.64 |
| Comp Mole Frac (Argon) | 0.00 | 0.00 | 0.00 | 0.00 | 0.00 | 0.00 | 0.00 | 0.01 | 0.01 |
| Comp Mole Frac ($H_2O$) | 0.00 | 1.00 | 0.12 | 0.00 | 0.12 | 0.00 | 0.03 | 0.01 | 0.35 |
| Comp Mole Frac (CO) | 0.00 | 0.00 | 0.02 | 0.00 | 0.00 | 0.00 | 0.00 | 0.00 | 0.00 |
| Comp Mole Frac ($CO_2$) | 0.00 | 0.00 | 0.20 | 0.00 | 0.23 | 0.00 | 0.71 | 0.00 | 0.00 |
| Comp Mole Frac (Ethane) | 0.00 | 0.00 | 0.00 | 0.00 | 0.00 | 0.00 | 0.00 | 0.00 | 0.00 |
| Comp Mole Frac (BiPhenyl) | 0.02 | 0.00 | 0.00 | 0.00 | 0.00 | 0.00 | 0.00 | 0.00 | 0.00 |

**Table 11. Utility Consumption and Net Total Power Generation of the Process**

| Utility | Value | Unit |
|---|---|---|
| Cooling Water | 32367.7 | kg/h |
| LP Steam | 4.1 | kg/h |
| MP Steam | 60.3 | kg/h |
| HP Steam | 41.5 | kg/h |
| Net Power Generation | 300 | kW |

(Table 12) compares the requirements for a purified hydrogen stream with the simulation results, highlighting the relative error for each component.

- Water: The simulation shows a 4% relative error, indicating a very close match to the requirement.
- Total Hydrocarbons: With a 5% relative error, the hydrocarbons are also very close to the required amount.
- Oxygen: The oxygen level in the simulation has a minimal deviation, with a 2% relative error.
- $CO_2$: The $CO_2$ level in the simulation shows a 10% relative error, which is slightly higher but still within an acceptable range.
- CO: The simulation matches the requirement exactly, resulting in a 0% relative error.
- Total Sulfur: The sulfur content has a relative error of 12.5%, indicating the need for some adjustment.

The average relative error across all components is 7.62%. This indicates that the simulation results are generally close to the required specifications for the purified hydrogen stream, with only minor deviations. The process appears to be well-calibrated, with the sulfur content being the only area requiring more attention.

**Table 12. Comparison of Simulation Results with Purified Hydrogen Stream Requirements**

| | Requirements for Purified Hydrogen Stream (µmol/mol) | Simulation (µmol/mol) | Relative Error, % |
|---|---|---|---|
| Water | 5 | 4.8 | 4 |
| Total Hydrocarbons | 2 | 1.9 | 5 |
| Oxygen | 5 | 4.9 | 2 |
| $CO_2$ | 2 | 1.8 | 10 |
| CO | 0.2 | 0.2 | 0 |
| Total Sulfur | 0.004 | 0.0035 | 12.5 |
| | Average Error | | 7.62 |

## 4.1. Environmental Impacts

Generating hydrogen, especially when $CO_2$ is emitted as a by-product, has notable environmental consequences. Evaluating the sustainability of hydrogen as an energy source depends heavily on this process. Hydrogen production via steam reforming of gas or liquid hydrocarbons releases significant $CO_2$, substantially contributing to global warming (Nowotny & Veziroglu, 2011). The retentate stream exiting the hydrogen purification unit ($CO_2$+$H_2$) enters the diesel reforming process. When combined with the diesel burned in the furnace, it generates a stack-gas, which acts as the conduit for all the $CO_2$ produced in the process. All the $CO_2$ is released through the stack-gas stream. (Table 13) provides the detailed specifications of the stack-gas stream, including its composition, temperature, pressure, and flow rate. This information is essential for understanding the environmental impact and efficiency of the process.

**Table 13. Stack-Gas Stream Specifications**

| Properties | Stack-Gas |
|---|---|
| Vapor Fraction | 1 |
| Temperature (°C) | 50 |
| Pressure (bar) | 1 |
| Molar flow (kgmole/h) | 4.63 |
| Mass Flow (kg/h) | 180.48 |
| Comp Mole Frac ($CO_2$) | 0.75 |
| Comp Mole Frac ($H_2O$) | 0.2 |
| Comp Mole Frac ($O_2$) | 0.05 |

In contrast, green hydrogen, produced using renewable energy sources, has a significantly lower environmental impact compared to hydrogen generated from fossil fuels (Amin et al., 2022). The environmental impact of hydrogen generation depends heavily on the production method. Fossil fuel-based methods, such as steam methane reforming, produce significant $CO_2$ emissions contributing to global warming. In contrast, green hydrogen production using renewable energy sources, coupled with $CO_2$ capture and storage technologies, can substantially reduce these emissions, making hydrogen a more sustainable energy source.

## 5. Conclusions

Hydrogen production faces significant challenges in transportation, making liquid fuel reforming an attractive solution. The ability to export liquid products efficiently and cost-effectively enhances the global accessibility of hydrogen. Utilizing process design software like Aspen HYSYS and PRO/II allows for efficient simulation and design of sour diesel fuel conversion processes, including membrane units. Liquid fuels, particularly diesel, offer promise for mid-term hydrogen production. However, developing a satisfactory hydrogen supply system remains critical for commercial viability. Diesel's attributes, including low cost, high hydrogen carrier potential, availability, ease of transportation, and high energy density, position it as an attractive option. Sulfur compounds in diesel must be removed before reforming to avoid catalyst poisoning. Steam reforming of liquid fuel offers a high hydrogen-to-carbon monoxide ratio, but carbon monoxide levels must be minimized, as they are toxic to catalysts and fuel cells. Fuel cells, with their high efficiency in converting chemical energy to electricity, provide a clean and efficient energy source. In a scenario where 63 kg/h of diesel is introduced into the process to produce 300 kW of net power from the fuel cell, the power consumption is 2.50 kW, with cooling water consumption at 32367 kg/h, LP steam consumption at 4.1 kg/h, MP steam consumption at 60.3 kg/h, and HP steam consumption at 41.5 kg/h. For future investigations, it is imperative to delve into advanced catalyst materials to optimize sulfur removal and reforming processes and explore innovative approaches for reducing carbon monoxide levels and enhancing the water-gas shift reaction. Developing integrated systems to maximize energy efficiency and minimize utility consumption should also be a priority. Furthermore, rigorous assessments of the scalability and economic viability of large-scale liquid fuel reforming processes, including ROI and Payback Period considerations, are essential. Lastly, there is a critical need to explore emerging technologies, such as hydrogen storage and distribution systems, to overcome existing hydrogen transportation and utilization challenges, ensuring a sustainable and economically viable energy future. Additionally, a more detailed comparison of hydrogen production from renewable sources and methods that do not produce secondary emissions (such as electrolysis) would be beneficial.

## References


Amin, M., Shah, H. H., Fareed, A. G., Khan, W. U., Chung, E., Zia, A., Farooqi, Z. U. R., & Lee, C. (2022). Hydrogen production through renewable and non-renewable energy processes and their impact on climate change. International Journal of Hydrogen Energy, 47(77), 33112-33134.

Amphlett, J. C., Mann, R. F., Peppley, B. A., Roberge, P. R., Rodrigues, A., & Salvador, J. P. (1998). Simulation of a 250 kW diesel fuel processor/PEM fuel cell system. Journal of Power Sources, 71(1-2), 179-184.

Awad, S. A., Gheni, S. A., Abdullah, G. H., & Ahmed, S. M. R. (2020). Design and evaluation of a Co-Mo-supported nano alumina ultradeep hydrodesulfurization catalyst for production of environmentally friendly diesel fuel in a trickle bed reactor. ACS Omega, 5(21), 12081-12089.

Bacquart, T., Arrhenius, K., Persijn, S., Rojo, A., Auprêtre, F., Gozlan, B., Moore, N., Morris, A., Fischer, A., & Murugan, A. (2019). Hydrogen fuel quality from two main production processes: Steam methane reforming and proton exchange membrane water electrolysis. Journal of Power Sources, 444, 227170.

Bae, J., Lee, S., Kim, S., Oh, J., Choi, S., Bae, M., Kang, I., & Katikaneni, S. P. (2016). Liquid fuel processing for hydrogen production: A review. International Journal of Hydrogen Energy, 41(44), 19990-20022.

Bae, M., Cheon, H., Oh, J., Kim, D., Bae, J., & Katikaneni, S. P. (2021). Rapid start-up strategy of 1 kWe diesel reformer by solid oxide fuel cell integration. International Journal of Hydrogen Energy, 46(52), 26575-26581.

Brown, L. F. (2001). A comparative study of fuels for on-board hydrogen production for fuel-cell-powered automobiles. International Journal of Hydrogen Energy, 26(4), 381-397.

Castaldi, M. J. (2009). Removal of trace contaminants from fuel processing reformate: preferential oxidation (Prox). Hydrogen and Syngas Production and Purification Technologies; Liu, K., Song, C., Subramani, V., Eds, 329-356.

Cherif, A., Nebbali, R., Sheffield, J. W., Doner, N., & Sen, F. (2021). Numerical investigation of hydrogen production via autothermal reforming of steam and methane over Ni/$Al_2O_3$ and Pt/$Al_2O_3$ patterned catalytic layers. International Journal of Hydrogen Energy, 46(75), 37521-37532.

Creaser, D., Karatzas, X., Lundberg, B., Pettersson, L. J., & Dawody, J. (2011). Modeling study of 5 kWe-scale autothermal diesel fuel reformer. Applied Catalysis A: General, 404(1-2), 129-140.

Davó-Quiṇonero, A., Bailon-Garcia, E., Lopez-Rodriguez, S., Juan-Juan, J., Lozano-Castello, D., García-Melchor, M., Herrera, F. C., Pellegrin, E., Escudero, C., & Bueno-Lopez, A. (2020). Insights into the oxygen vacancy filling mechanism in CuO/$CeO_2$ catalysts: a key step toward high selectivity in preferential CO oxidation. ACS Catalysis, 10(11), 6532-6545.

Dawood, F., Anda, M., & Shafiullah, G. M. (2020). Hydrogen production for energy: An overview. International Journal of Hydrogen Energy, 45(7), 3847-3869.

Dolanc, G., Pregelj, B., Petrovčič, J., Pasel, J., & Kolb, G. (2016). Control of autothermal reforming reactor of diesel fuel. Journal of Power Sources, 313, 223-232.

Douglas, J. M. (1988). Conceptual design of chemical processes. (No Title).

Ersoz, A., Olgun, H., & Ozdogan, S. (2006). Reforming options for hydrogen production from fossil fuels for PEM fuel cells. Journal of Power Sources, 154(1), 67-73.

Fauteux-Lefebvre, C., Abatzoglou, N., Braidy, N., & Achouri, I. E. (2011). Diesel steam reforming with a nickel-alumina spinel catalyst for solid

oxide fuel cell application. Journal of Power Sources, 196(18), 7673-7680.

Geng, J., Guo, Q., Pan, J., Chi, B., & Pu, J. (2023). Enhanced stability of co-reforming diesel and methanol into hydrogen-enriched gases for solid oxide fuel cell application. Journal of Power Sources, 564, 232830.

Ghasemzadeh, K., Jafari, M., & Basile, A. (2017). Theoretical Study of Various Configurations of Membrane Processes for Olefins Separation. International Journal of Membrane Science and Technology, 4, 1-7.

Gonzalez, A. M., Lora, E. E. S., Palacio, J. C. E., & del Olmo, O. A. A. (2018). Hydrogen production from oil sludge gasification/biomass mixtures and potential use in hydrotreatment processes. International Journal of Hydrogen Energy, 43(16), 7808-7822.

Hoguet, J.-C., Karagiannakis, G. P., Valla, J. A., Agrafiotis, C. C., & Konstandopoulos, A. G. (2009). Gas and liquid phase fuels desulphurization for hydrogen production via reforming processes. International Journal of Hydrogen Energy, 34(11), 4953-4962.

Jafari, M., Deljoo, M. S., & Vatani, A. (2020). Simulation and Economic Evaluation of Polygeneration System for Coproduction of Power, Steam, $CH_3OH$, $H_2$, and $CO_2$ from Flare Gas. Iranian Journal of Oil and Gas Science and Technology, 9(4), 93-114. https://doi.org//10.22050/ijogst.2020.227023.1547

Jafari, M., & Garakani, A. K. (2021). Simulation and techno-economic analysis of hydrotreating process of mazut. Journal of Applied Research of Chemical-Polymer Engineering, 5(1), 17-30.

Jafari, M., & Khalili-Garakani, A. (2021). Techno-Economic Analysis of Heavy Fuel Oil Hydrodesulfurization Process for Application in Power Plants. Iranian Journal of Oil and Gas Science and Technology, 10(1), 40-65.

Jafari, M., Sarrafzadeh, M. H., & Deljoo, M. S. (2021). Economic Evaluation of Water Desalination and Power Generation Using Flare Gases of Assaluyeh. Iranian Journal of Gas Engineering, 8(1), 7-17. https://www.ijge.irangi.org/article_251915.html

Jafari, M., Sarrafzadeh, M.-H., & Ghasemzadeh, K. (2020). Simulation and economic evaluation of heat and power generation from flare gases in a combined cycle power plant. Energy Equipment and Systems, 8(4), 307-322.

Jafari, M., Vatani, A., Deljoo, M. S., & Khalili-Garakani, A. (2021). Techno-Economic Analysis of Flare Gas to Gasoline (FGTG) Process through Dimethyl Ether Production. Journal of Gas Technology, 6(2), 28-44. https://doi.org//jgt.irangi.org/article_251676.html

Jejurkar, S. Y., Khanna, A., & Verma, N. (2020). Maldistribution effects in an industrial-scale trickle bed reactor. Industrial & Engineering Chemistry Research, 59(16), 7405-7415.

Ješić, D., Erklavec Zajec, V., Bajec, D., Dolanc, G., Berčič, G., & Likozar, B. (2022). Computational investigation of auto-thermal reforming process of diesel for production of hydrogen for PEM fuel cell applications. International Journal of Energy Research, 46(12), 17068-17083.

Kaila, R. K., Gutiérrez, A., & Krause, A. O. I. (2008). Autothermal reforming of simulated and commercial diesel: The performance of zirconia-supported RhPt catalyst in the presence of sulfur. Applied Catalysis B: Environmental, 84(1-2), 324-331.

Le, T. T., Sharma, P., Bora, B. J., Tran, V. D., Truong, T. H., Le, H. C., & Nguyen, P. Q. P. (2023). Fueling the future: A comprehensive review of hydrogen energy systems and their challenges. International Journal of Hydrogen Energy.

Lee, Y.-L., Kim, K.-J., Hong, G.-R., & Roh, H.-S. (2023). Target-oriented water-gas shift reactions with customized reaction conditions and catalysts. Chemical Engineering Journal, 458, 141422.

Lindermeir, A., Kah, S., Kavurucu, S., & Mühlner, M. (2007). On-board diesel fuel processing for an SOFC-APU-Technical challenges for catalysis and reactor design. Applied Catalysis B: Environmental, 70(1-4), 488-497.

Lindström, B., Karlsson, J. A. J., Ekdunge, P., De Verdier, L., Häggendal, B., Dawody, J., Nilsson, M., & Pettersson, L. J. (2009). Diesel fuel reformer for automotive fuel cell applications. International Journal of Hydrogen Energy, 34(8), 3367-3381.

Liu, D.-J., Kaun, T. D., Liao, H.-K., & Ahmed, S. (2004). Characterization of kilowatt-scale autothermal reformer for production of hydrogen from heavy hydrocarbons. International Journal of Hydrogen Energy, 29(10), 1035-1046.

Martin, S., Kraaij, G., Ascher, T., Baltzopoulou, P., Karagiannakis, G., Wails, D., & Wörner, A. (2015). Direct steam reforming of diesel and diesel-biodiesel blends for distributed hydrogen generation. International Journal of Hydrogen Energy, 40(1), 75-84.

Nowotny, J., & Veziroglu, T. N. (2011). Impact of hydrogen on the environment. International Journal of Hydrogen Energy, 36(20), 13218-13224.

Pereira, C., Bae, J. M., Ahmed, S., & Krumpelt, M. (2000). Liquid fuel reformer development: autothermal reforming of diesel fuel. Argonne National Lab., IL (US).

Permatasari, A., Fasahati, P., Ryu, J.-H., & Liu, J. J. (2016). Design and analysis of a diesel processing unit for a molten carbonate fuel cell for auxiliary power unit applications. Korean Journal of Chemical Engineering, 33, 3381-3387.

Ramantani, T., Evangeliou, V., Kormentzas, G., & Kondarides, D. I. (2022). Hydrogen production by steam reforming of propane and LPG over supported metal catalysts. Applied Catalysis B: Environmental, 306, 121129.

Sahin, Z. (2008). Experimental and theoretical investigation of the effects of gasoline blends on single-cylinder diesel engine performance and exhaust emissions. Energy & Fuels, 22(5), 3201-3212.

Samsun, R. C., Pasel, J., Peters, R., & Stolten, D. (2015). Fuel cell systems with reforming of petroleum-based and synthetic-based diesel and kerosene fuels for APU applications. International Journal of Hydrogen Energy, 40(19), 6405-6421.

Samsun, R. C., Prawitz, M., Tschauder, A., Meißner, J., Pasel, J., & Peters, R. (2020). Reforming of diesel and jet fuel for fuel cells on a systems level: Steady-state and transient operation. Applied Energy, 279, 115882.

Wang, H., Zhao, H., & Zhao, Z. (2021). Thermodynamic performance study of a new SOFC-CCHP system with diesel reforming by CLHG to produce hydrogen as fuel. International Journal of Hydrogen Energy, 46(44), 22956-22973.

# طراحی و شبیه‌سازی تولید هیدروژن از ریفرمینگ دیزل برای کاربردهای پیل سوختی


- مصطفی جعفری[۱]، مجید خورشیدیان[۲*]، مظاهر رحیمی اسبوئی[۳]، وحید کرد فیروزجائی[۲]، علی وطنی[۴]

۱. پژوهشگر، موسسه گاز طبیعی مایع (I-LNG)، دانشکده مهندسی شیمی، دانشکده فنی، دانشگاه تهران، تهران، ایران

۲. پژوهشگر، دانشگاه صنعتی مالک اشتر، پژوهشکده علوم و فناوری شمال، فریدونکنار، ایران

۳. استادیار، دانشگاه صنعتی مالک اشتر، پژوهشکده علوم و فناوری شمال، فریدونکنار، ایران

۴. استاد، موسسه گاز طبیعی مایع (I-LNG)، دانشکده مهندسی شیمی، دانشکده فنی، دانشگاه تهران، تهران، ایران

(ایمیل نویسنده مسئول: khorshidian@mut.ac.ir)


## چکیـــــــده


تولید هیدروژن با چالش‌های قابل توجهی در حمل و نقل و ذخیره‌سازی مواجه است، مانند نشت، ایمنی در حین انتقال و نیاز به شرایط ذخیره‌سازی کارآمد. تولید در محل از طریق ریفرمینگ سوخت دیزل یک راه‌حل امیدوارکننده به شمار می‌رود به دلیل مقرون‌به‌صرفه بودن، دسترسی آسان و سهولت حمل و نقل دیزل. با این حال، گوگرد و مونوکسید کربن موجود در دیزل باید حذف شوند تا از کاتالیزورهای دخیل در این فرآیند محافظت شود. این مطالعه یک فرآیند مفهومی برای ریفرمینگ دیزل حاوی گوگرد به‌منظور تولید ۳۰۰ کیلووات برق در یک سیستم پیل سوختی را با استفاده از روش داگلاس طراحی می‌کند، که طراحی فرآیند شیمیایی را به یک سلسله مراتب تصمیم‌گیری سازماندهی می‌کند. این سلسله مراتب با ساختار ورودی-خروجی شروع می‌شود و فرآیند را با جزئیات دادن به جریان‌های ورودی و خروجی بر اساس متغیرهای طراحی تعیین شده خلاصه می‌کند. ساختار جریان بازیافتی فرآیند را به بخش‌های راکتور و جداسازی تقسیم می‌کند، که هر کدام جریان‌های بازیافتی تعریف شده‌ای را در برمی‌گیرند. در نهایت، ساختار کلی بخش جداسازی، سیستم‌های بازیافت گاز و مایع را ادغام می‌کند و یک استراتژی جامع برای طراحی واحدهای جداسازی ارائه می‌دهد. نمودار جریان فرآیند (PFD) ابتدا توسعه یافت و سپس از طریق شبیه‌سازی با استفاده از نرم‌افزار Aspen HYSYS به‌دقت تحلیل شد. نتایج نشان می‌دهد که تولید ۳۰۰ کیلووات برق به ۱۷ کیلوگرم در ساعت هیدروژن خالص نیاز دارد که مستلزم ۴۷ کیلوگرم در ساعت دیزل بدون گوگرد است. به‌طور کلی، ۶۰ کیلوگرم در ساعت دیزل مورد نیاز است. تحقیقات آینده باید بر بهینه‌سازی حذف گوگرد، کاهش سطح مونوکسید کربن، بهبود واکنش تغییر آب-گاز، به حداکثر رساندن بهره‌وری انرژی و ارزیابی قابلیت اقتصادی، از جمله بازگشت سرمایه و دوره بازپرداخت، متمرکز شود.


**واژگان کلیدی:** دیزل، ریفرمینگ، هیدروژن، سلول سوختی، برق، اسپن هایسیس